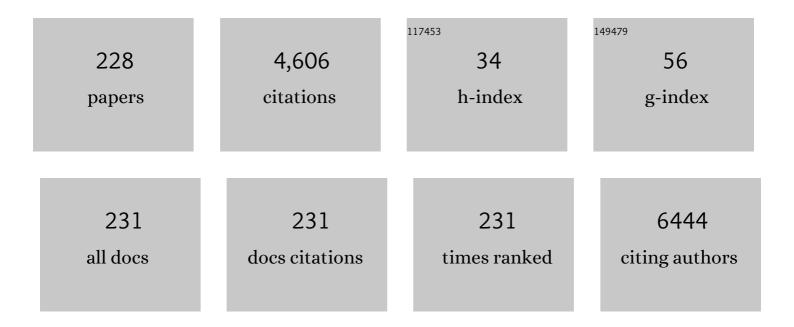
## Saulius Kaciulis

List of Publications by Year in descending order

Source: https://exaly.com/author-pdf/7118218/publications.pdf Version: 2024-02-01



#	Article	IF	CITATIONS
1	Tuneable properties of carbon quantum dots by different synthetic methods. Journal of Nanostructure in Chemistry, 2022, 12, 565-580.	5.3	27
2	Silver@Hydroxyapatite functionalized calcium carbonate composites: characterization, antibacterial and antibiofilm activities and cytotoxicity. Applied Surface Science, 2022, 586, 152760.	3.1	12
3	Metal Surfaces. Coatings, 2021, 11, 255.	1.2	Ο
4	Three-Dimensional X-ray Imaging of $\hat{l}^2$ -Galactosidase Reporter Activity by Micro-CT: Implication for Quantitative Analysis of Gene Expression. Brain Sciences, 2021, 11, 746.	1.1	8
5	Hydroxyapatite Functionalized Calcium Carbonate Composites with Ag Nanoparticles: An Integrated Characterization Study. Nanomaterials, 2021, 11, 2263.	1.9	7
6	Zn–Al Layered Double Hydroxides Synthesized on Aluminum Foams for Fluoride Removal from Water. Processes, 2021, 9, 2109.	1.3	2
7	Extra-Low Dosage Graphene Oxide Cementitious Nanocomposites: A Nano- to Macroscale Approach. Nanomaterials, 2021, 11, 3278.	1.9	10
8	Aluminum (Oxy)nitride thin films grown by fs-PLD as electron emitters for thermionic applications. AIP Conference Proceedings, 2021, , .	0.3	6
9	Influence of iron and nitrogen ion beam exposure on the gas sensing properties of CuO nanowires. Sensors and Actuators B: Chemical, 2020, 321, 128579.	4.0	16
10	ESCA as a Tool for Exploration of Metals' Surface. Coatings, 2020, 10, 1182.	1.2	7
11	Effect of mercapto-silanes on the functional properties of highly amorphous vinyl alcohol composites with reduced graphene oxide and cellulose nanocrystals. Composites Science and Technology, 2020, 200, 108458.	3.8	14
12	Cr Segregation and Impact Fracture in a Martensitic Stainless Steel. Coatings, 2020, 10, 843.	1.2	14
13	Rhodium as efficient additive for boosting acetone sensing by TiO2 nanocrystals. Beyond the classical view of noble metal additives. Sensors and Actuators B: Chemical, 2020, 319, 128338.	4.0	6
14	La distribution on the crater surface of Wâ€4%La 2 O 3 produced by a single laser pulse. Surface and Interface Analysis, 2020, 52, 1093-1097.	0.8	1
15	XPS study of Cr segregation in a martensitic stainless steel. Surface and Interface Analysis, 2020, 52, 1089-1092.	0.8	3
16	Photovoltaic Anodes for Enhanced Thermionic Energy Conversion. ACS Energy Letters, 2020, 5, 1364-1370.	8.8	35
17	Correlation between the bath composition and nanoporosity of DCâ€electrodeposited Niâ€Fe alloy. Surface and Interface Analysis, 2020, 52, 907-913.	0.8	0
18	Adsorption of heavy metals by layered double hydroxides grown in situ on Al foam. Surface and Interface Analysis, 2020, 52, 996-999.	0.8	2

#	Article	IF	CITATIONS
19	Xâ€ray and UV photoelectron spectroscopy of Ag nanoclusters. Surface and Interface Analysis, 2020, 52, 1017-1022.	0.8	18
20	Work function and negative electron affinity of ultrathin barium fluoride films. Surface and Interface Analysis, 2020, 52, 968-974.	0.8	4
21	Nanocrystalline lanthanum boride thin films by femtosecond pulsed laser deposition as efficient emitters in hybrid thermionic-photovoltaic energy converters. Applied Surface Science, 2020, 513, 145829.	3.1	17
22	Surface and structural analysis of epitaxial La 1â^' x Sr x (Mn 1â^' y Co y ) z O 3 films. Surface and Interface Analysis, 2020, 52, 900-906.	0.8	2
23	Ultra-thin films of barium fluoride with low work function for thermionic-thermophotovoltaic applications. Materials Chemistry and Physics, 2020, 249, 122989.	2.0	10
24	Fluorescence enhancement induced by the interaction of silver nanoclusters with lead ions in water. Colloids and Surfaces A: Physicochemical and Engineering Aspects, 2019, 579, 123634.	2.3	21
25	Room temperature Co-doped manganite/graphene sensor operating at high pulsed magnetic fields. Scientific Reports, 2019, 9, 9497.	1.6	11
26	Lead-Bismuth Eutectic: Atomic and Micro-Scale Melt Evolution. Materials, 2019, 12, 3158.	1.3	2
27	High piezo-resistive performances of anisotropic composites realized by embedding rGO-based chitosan aerogels into open cell polyurethane foams. Nanoscale, 2019, 11, 8835-8844.	2.8	33
28	Lanthanum (oxy)boride thin films for thermionic emission applications. Applied Surface Science, 2019, 479, 296-302.	3.1	16
29	Graphene quantum dots obtained by unfolding fullerene. Thin Solid Films, 2019, 673, 19-25.	0.8	22
30	Reduction of graphene oxide by UHV annealing. Surface and Interface Analysis, 2018, 50, 1089-1093.	0.8	9
31	Surface phenomena during the early stage of liquid phase SPS of a mixture of coarse WC and Niâ€alloy particles. Surface and Interface Analysis, 2018, 50, 1072-1076.	0.8	0
32	Oxidative treatment effect on TiH <sub>2</sub> powders. Surface and Interface Analysis, 2018, 50, 1195-1199.	0.8	4
33	Piezoelectric Thin Films of ZnO-Nanorods/Nanowalls Grown by Chemical Bath Deposition. IEEE Nanotechnology Magazine, 2018, 17, 311-319.	1.1	23
34	Surface and microstructural analyses of a Roman quadrans dating back to first century <scp>ad</scp> . Surface and Interface Analysis, 2018, 50, 1042-1045.	0.8	1
35	Nanocluster superstructures or nanoparticles? The self-consuming scaffold decides. Nanoscale, 2018, 10, 7472-7483.	2.8	17
36	Low-temperature titania coatings for aluminium corrosion protection. Corrosion Engineering Science and Technology, 2018, 53, 44-53.	0.7	5

#	Article	IF	CITATIONS
37	Resin-Based Materials with Chlorhexidine-Loaded MCM-41: Surface Characteristics, Drug Release, and Antibiofilm Activity. ACS Biomaterials Science and Engineering, 2018, 4, 4144-4153.	2.6	6
38	Discriminating between Different Heavy Metal Ions with Fullerene-Derived Nanoparticles. Sensors, 2018, 18, 1496.	2.1	29
39	Preparation, intercalation, and characterization of nanostructured (Zn, Al) layered double hydroxides (LDHs). Surface and Interface Analysis, 2018, 50, 1094-1098.	0.8	8
40	Investigation of work function and chemical composition of thin films of borides and nitrides. Surface and Interface Analysis, 2018, 50, 1138-1144.	0.8	21
41	Bottom-Up Electrochemical Deposition of Poly(styrene sulfonate) on Nanoarchitectured Electrodes. ACS Applied Materials & Interfaces, 2017, 9, 22902-22910.	4.0	24
42	Galvanic Displaced Nickel-Silicon and Copper-Silicon Interfaces: A DFT Investigation. ECS Transactions, 2017, 75, 7-13.	0.3	1
43	Inorganic Photocatalytic Enhancement: Activated RhB Photodegradation by Surface Modification of SnO2 Nanocrystals with V2O5-like species. Scientific Reports, 2017, 7, 44763.	1.6	17
44	Thermoelectric Analysis of ZnSb Thin Films Prepared by ns-Pulsed Laser Deposition. Journal of Nanoscience and Nanotechnology, 2017, 17, 1564-1570.	0.9	2
45	Bridging spatially segregated redox zones with a microbial electrochemical snorkel triggers biogeochemical cycles in oil-contaminated River Tyne (UK) sediments. Water Research, 2017, 127, 11-21.	5.3	30
46	Solvothermal Synthesis, Gasâ€5ensing Properties, and Solar Cellâ€Aided Investigation of TiO <sub>2</sub> –MoO <sub>x</sub> Nanocrystals. ChemNanoMat, 2017, 3, 798-807.	1.5	2
47	Growth and characterization of ultrathin carbon films on electrodeposited Cu and Ni. Surface and Interface Analysis, 2017, 49, 1088-1094.	0.8	7
48	ZnSb-based thin films prepared by ns-PLD for thermoelectric applications. Applied Surface Science, 2017, 418, 589-593.	3.1	15
49	Surface immobilization of functional molecules by reactive selfâ€assembling. Surface and Interface Analysis, 2016, 48, 626-629.	0.8	Ο
50	Welding of IN792 DS superalloy by electron beam. Surface and Interface Analysis, 2016, 48, 483-487.	0.8	6
51	Investigation of graphene layers on electrodeposited polycrystalline metals. Surface and Interface Analysis, 2016, 48, 456-460.	0.8	7
52	Surface spectroscopy and structural analysis of nanostructured multifunctional (Zn, Al) layered double hydroxides. Surface and Interface Analysis, 2016, 48, 514-518.	0.8	31
53	Ceramic coatings for orthopaedic implants: preparation and characterization. Surface and Interface Analysis, 2016, 48, 616-620.	0.8	3
54	Effect of Heat Treatments on TiH <sub>2</sub> : Surface Composition and Hydrogen Release. Materials Science Forum, 2016, 879, 2032-2037.	0.3	2

#	Article	IF	CITATIONS
55	Fabrication of Graphene–Alumina Heterostructured Films with Nanotube Morphology. Journal of Physical Chemistry C, 2016, 120, 9490-9497.	1.5	13
56	Control of the size and density of ZnO-nanorods grown onto graphene nanoplatelets in aqueous suspensions. RSC Advances, 2016, 6, 83217-83225.	1.7	17
57	CHEMICAL COMPOSITION STUDY OF VANADIUM PENTOXIDE XEROGELS DOPED BY BOVINE ALBUMIN. Surface Review and Letters, 2016, 23, 1650058.	0.5	Ο
58	IN792 DS Superalloy: Optimization of EB Welding and Post-Welding Heat Treatments. Materials Science Forum, 2016, 879, 175-180.	0.3	4
59	Study of steelâ€WC interface produced by solidâ€state capacitor discharge sinterâ€welding. Surface and Interface Analysis, 2016, 48, 538-542.	0.8	10
60	Investigation of skin-core joints in aluminium foam sandwich panels by EDS and XPS. Surface and Interface Analysis, 2016, 48, 479-482.	0.8	1
61	Vapour phase nucleation of ZnO nanowires on GaN: growth habit, interface study and optical properties. RSC Advances, 2016, 6, 15087-15093.	1.7	6
62	Magnetic hydroxyapatite coatings as a new tool in medicine: A scanning probe investigation. Materials Science and Engineering C, 2016, 62, 444-449.	3.8	26
63	Tuning hard and soft magnetic FePt nanocomposites. Journal of Alloys and Compounds, 2016, 663, 601-609.	2.8	10
64	The "Oil-Spill Snorkelâ€: an innovative bioelectrochemical approach to accelerate hydrocarbons biodegradation in marine sediments. Frontiers in Microbiology, 2015, 6, 881.	1.5	60
65	Synthesis and characterization of ZnO nanorods with a narrow size distribution. RSC Advances, 2015, 5, 49861-49870.	1.7	49
66	High resolution surface characterization of chromophore-modified graphene. , 2015, , .		0
67	Effect of substrate temperature on the arrangement of ultra-thin TiO2 films grown by a dc-magnetron sputtering deposition. Thin Solid Films, 2015, 585, 5-12.	0.8	28
68	Highly conductive multilayer-graphene paper as a flexible lightweight electromagnetic shield. Carbon, 2015, 89, 260-271.	5.4	122
69	Tough and adhesive nanostructured calcium phosphate thin films deposited by the pulsed plasma deposition method. RSC Advances, 2015, 5, 78561-78571.	1.7	26
70	Nano-crystalline Ag–PbTe thermoelectric thin films by a multi-target PLD system. Applied Surface Science, 2015, 336, 283-289.	3.1	21
71	Electron spectroscopy of rubber and resin-based composites containing 2D carbon. Thin Solid Films, 2015, 581, 80-85.	0.8	16
72	Microchemical inhomogeneity in eutectic Pb–Bi alloy quenched from melt. Surface and Interface Analysis, 2014, 46, 877-881.	0.8	2

#	Article	IF	CITATIONS
73	Corrosion effect to the surface of stainless steel treated by two processes of low temperature carburization. Surface and Interface Analysis, 2014, 46, 731-734.	0.8	6
74	Micro hemical investigation of thick W coating on AISI 420 martensitic steel. Surface and Interface Analysis, 2014, 46, 873-876.	0.8	1
75	HT-XRD Analysis of W Thick Coatings for Nuclear Fusion Technology. Key Engineering Materials, 2014, 605, 31-34.	0.4	1
76	Influence of low-temperature carburising on metal release from AISI316L austenitic stainless steel in acetic acid. Journal of Food Engineering, 2014, 137, 7-15.	2.7	6
77	AlN thin films prepared by ArF plasma assisted PLD. Role of process conditions on electronic and chemical–morphological properties. Applied Physics A: Materials Science and Processing, 2014, 114, 611-617.	1.1	2
78	Quantum dots as mediators in gas sensing: A case study of CdS sensitized WO3 sensing composites. Applied Surface Science, 2014, 290, 295-300.	3.1	5
79	Electron spectroscopy of the main allotropes of carbon. Surface and Interface Analysis, 2014, 46, 966-969.	0.8	53
80	Hydrophobizing coatings for cultural heritage. A detailed study of resin/stone surface interaction. Applied Physics A: Materials Science and Processing, 2014, 116, 341-348.	1.1	43
81	Chitosan films containing mesoporous SBA-15 supported silver nanoparticles for wound dressing. Journal of Materials Chemistry B, 2014, 2, 6054.	2.9	75
82	The role of reduced graphene oxide on chemical, mechanical and barrier properties of natural rubber composites. Composites Science and Technology, 2014, 102, 74-81.	3.8	113
83	Fs-pulsed laser deposition of PbTe and PbTe/Ag thermoelectric thin films. Applied Physics A: Materials Science and Processing, 2014, 117, 401-407.	1.1	11
84	Ion release and tarnishing behavior of Au and Pd based amorphous alloys in artificial sweat. Corrosion Science, 2013, 77, 135-142.	3.0	6
85	Fabrication of SiGe rings and holes on Si(001) by flash annealing. Applied Surface Science, 2013, 283, 813-819.	3.1	4
86	Ceria/stannate multilayer coatings on AZ91D Mg alloy. Surface and Coatings Technology, 2012, 206, 4855-4863.	2.2	21
87	Relation between the microstructure and microchemistry in Niâ€based superalloy. Surface and Interface Analysis, 2012, 44, 982-985.	0.8	10
88	Spectroscopy of carbon: from diamond to nitride films. Surface and Interface Analysis, 2012, 44, 1155-1161.	0.8	163
89	Surface modification of austenitic steels by lowâ€ŧemperature carburization. Surface and Interface Analysis, 2012, 44, 1001-1004.	0.8	14
90	Influence of process conditions on chemical composition and electronic properties of AlN thin films prepared by ArF reactive pulsed laser deposition. Physica Status Solidi C: Current Topics in Solid State Physics, 2012, 9, 1053-1056.	0.8	1

6

#	Article	IF	CITATIONS
91	Structural, chemical, and electrical characterization of indium nitride produced by pulsed laser ablation. Physica Status Solidi C: Current Topics in Solid State Physics, 2012, 9, 993-996.	0.8	2
92	One-step substrate nanofabrication and patterning of nanoparticles by lithographically controlled etching. Nanotechnology, 2011, 22, 355301.	1.3	5
93	Critical Temperature Enhancement by Biaxial Compressive Strain in FeSe0.5Te0.5 Thin Films. Journal of Superconductivity and Novel Magnetism, 2011, 24, 35-41.	0.8	21
94	Carbon nitride films by RF plasma assisted PLD: Spectroscopic and electronic analysis. Applied Surface Science, 2011, 257, 5175-5180.	3.1	14
95	Effect of composition on mechanical behaviour of diamond-like carbon coatings modified with titanium. Thin Solid Films, 2011, 519, 3061-3067.	0.8	25
96	Effect of deposition temperature on chemical composition and electronic properties of amorphous carbon nitride (a-CNx) thin films grown by plasma assisted pulsed laser deposition. Thin Solid Films, 2011, 519, 4059-4063.	0.8	20
97	Influence of PECVD parameters on the properties of diamond-like carbon films. Thin Solid Films, 2011, 519, 4087-4091.	0.8	61
98	Comparison between Roll Diffusion Bonding and Hot Isostatic Pressing Production Processes of Ti6Al4V-SiC <sub>f</sub> Metal Matrix Composites. Materials Science Forum, 2011, 678, 145-154.	0.3	6
99	Chemical composition of superconducting SmFeAsO doped with fluorine. Surface and Interface Analysis, 2010, 42, 692-695.	0.8	2
100	Microchemical characterisation of carbon–metal interface in Ti6Al4Vi£¿SiC <sub>f</sub> composites. Surface and Interface Analysis, 2010, 42, 707-711.	0.8	8
101	XPS study of gold-based metallic glass. Surface and Interface Analysis, 2010, 42, 597-600.	0.8	8
102	Structure and composition of electrospun titania nanofibres doped with Eu. Surface and Interface Analysis, 2010, 42, 572-575.	0.8	22
103	Composition of plasmaâ€sprayed tungsten coatings on CuCrZr alloy. Surface and Interface Analysis, 2010, 42, 1197-1200.	0.8	10
104	Heating modification of an austenitic steel with highâ€nitrogen content. Surface and Interface Analysis, 2010, 42, 726-729.	0.8	9
105	Surface investigation of carbon films: from diamond to graphite. Surface and Interface Analysis, 2010, 42, 1082-1084.	0.8	149
106	Anelastic Phenomena at the Fibre-Matrix Interface of the Ti6Al4V-SiC <sub>f</sub> Composite. Key Engineering Materials, 2010, 425, 263-270.	0.4	3
107	Discontinuous Precipitation in a High-Nitrogen Austenitic Steel. Materials Science Forum, 2010, 638-642, 3597-3602.	0.3	5
108	High Yield Synthesis of Pure Alkanethiolate-Capped Silver Nanoparticles. Langmuir, 2010, 26, 15561-15566.	1.6	32

7

#	Article	IF	CITATIONS
109	Ordered arrays of FePt nanoparticles on unoxidized silicon surface by wet chemistry. Superlattices and Microstructures, 2009, 46, 95-100.	1.4	10
110	The metals chemical states in hydrated vanadium oxides. Micron, 2009, 40, 126-129.	1.1	5
111	Supramolecular Colloidal Systems of Gold Nanoparticles/Amphiphilic Cyclodextrin: a FE-SEM and XPS Investigation of Nanostructures Assembled onto Solid Surface. Journal of Physical Chemistry C, 2009, 113, 12772-12777.	1.5	37
112	Chemical composition of magnesium boride films obtained by CVD. Surface and Interface Analysis, 2008, 40, 741-745.	0.8	7
113	Composite of Ti6Al4V and SiC fibres: evolution of fibre–matrix interface during heat treatments. Surface and Interface Analysis, 2008, 40, 277-280.	0.8	15
114	Nanowires of metal oxides for gas sensing applications. Surface and Interface Analysis, 2008, 40, 575-578.	0.8	31
115	Effect of oxygen partial pressure on PLD cobalt oxide films. Applied Surface Science, 2008, 254, 5111-5115.	3.1	29
116	Chemical vapor deposition of hafnium dioxide thin films from cyclopentadienyl hafnium compounds. Thin Solid Films, 2008, 516, 7354-7360.	0.8	4
117	XPS analysis of several zeolitic and clay-based nanoporous materials for C4 hydrocarbon conversions. Microporous and Mesoporous Materials, 2008, 110, 64-71.	2.2	12
118	Doped ZnO nanowires: Towards homojuctions. , 2008, , .		1
119	Hydrogen Gas Sensing Performance Of Pt/Sno <sub>2</sub> Nanowires/Sic Mos Devices. International Journal on Smart Sensing and Intelligent Systems, 2008, 1, 771-783.	0.4	15
120	XPS and optical properties of sol-gel processed vanadium pentoxide films. Lithuanian Journal of Physics, 2008, 48, 341-348.	0.1	10
121	ANCHORAGE OF AMPHIPHILIC CYCLODEXTRINS WITH GOLD NANOPARTICLES ON SOLID SUBSTRATES. , 2008, , .		0
122	Preparation and Characterization of Tin Oxide Nanowires on SIC. , 2007, , .		1
123	Study of Magnesium Boride Films Obtained From Mg(BH <sub>4</sub> ) <sub>2</sub> by CVD. Chemical Vapor Deposition, 2007, 13, 414-419.	1.4	10
124	Growth of Hafnium Dioxide Thin Films by MOCVD Using a New Series of Cyclopentadienyl Hafnium Compounds. Chemical Vapor Deposition, 2007, 13, 626-632.	1.4	16
125	Zirconia primers for corrosion resistant coatings. Surface and Coatings Technology, 2007, 201, 5822-5828.	2.2	85
126	Deposition of Ti-containing diamond-like carbon (DLC) films by PECVD technique. Materials Science and Engineering C, 2007, 27, 1328-1330.	3.8	49

#	Article	IF	CITATIONS
127	Feasibility of enzyme biosensors based on gold nanowires. Materials Science and Engineering C, 2007, 27, 1158-1161.	3.8	23
128	Preparation and characterization of Fe-MCM-41 catalysts employed in the degradation of plastic materials. Microporous and Mesoporous Materials, 2007, 99, 140-148.	2.2	67
129	Correlation between atomic composition and gas sensing properties in tungsten–iron oxide thin films. Sensors and Actuators B: Chemical, 2007, 127, 22-28.	4.0	17
130	Carburisation layers for the growth of silicon carbide on silicon. , 2006, , .		0
131	Evolution of the Pt Layer Deposited on MgO(001) by Pulsed Laser Deposition as a Function of the Deposition Parameters:Â A Scanning Tunneling Microscopy and Energy Dispersive X-ray Diffractometry/Reflectometry Study. Journal of Physical Chemistry B, 2006, 110, 5529-5536.	1.2	15
132	Immobilization of GOD and HRP enzymes on nanostructured substrates. Surface and Interface Analysis, 2006, 38, 478-481.	0.8	27
133	XPS investigation of CoOx-based MRISiC structures for hydrocarbon gas sensing. Surface and Interface Analysis, 2006, 38, 736-739.	0.8	20
134	Characterization of Ohmic contacts on GaN/AlGaN heterostructures. Applied Surface Science, 2006, 253, 1055-1064.	3.1	4
135	Influence of electrodes ageing on the properties of the gas sensors based on SnO2. Sensors and Actuators B: Chemical, 2006, 115, 396-402.	4.0	20
136	Properties of the planar ADH-dry-layer structures based on electrically controlled coupling between enzyme molecules and metal surfaces. Sensors and Actuators B: Chemical, 2006, 118, 60-66.	4.0	2
137	Multi-technique study of corrosion resistant CrN/Cr/CrN and CrN:C coatings. Surface and Coatings Technology, 2006, 201, 313-319.	2.2	39
138	SAW-based gas sensors with rf sputtered InOx and PECVD SiNx films: Response to H2 and O3 gases. Sensors and Actuators B: Chemical, 2006, 118, 362-367.	4.0	23
139	Third-generation biosensors based on TiO2 nanostructured films. Materials Science and Engineering C, 2006, 26, 947-951.	3.8	89
140	Comparative study of surface acoustic wave based hydrogen sensors with: InO x /SiN x /36° YX LiTaO 3 structure. , 2005, 6035, 333.		0
141	Gold nanotubules arrays as new materials for sensing and biosensing: Synthesis and characterization. Sensors and Actuators B: Chemical, 2005, 111-112, 526-531.	4.0	41
142	Tuning of the response kinetics by the impurity concentration in metal oxide gas sensors. Sensors and Actuators B: Chemical, 2005, 111-112, 36-44.	4.0	8
143	Lead enrichment at the surface of lead zirconate titanate thin films. Journal of the European Ceramic Society, 2005, 25, 2495-2498.	2.8	23
144	Structural and dielectric properties of ZrTiO4 and Zr0.8Sn0.2TiO4 deposited by pulsed laser deposition. Materials Science and Engineering B: Solid-State Materials for Advanced Technology, 2005, 118, 87-91.	1.7	14

#	Article	IF	CITATIONS
145	Characterization of composite titanium nitride coatings prepared by reactive plasma spraying. Electrochimica Acta, 2005, 50, 4531-4537.	2.6	62
146	A Comparative Study of Cr2O3 Thin Films Obtained by MOCVD using Three Different Precursors. Chemical Vapor Deposition, 2005, 11, 375-380.	1.4	43
147	"Gold corrosion― red stains on a gold Austrian Ducat. Applied Physics A: Materials Science and Processing, 2004, 79, 205-211.	1.1	23
148	Depth profiling of thin films of binary metal oxides. Surface and Interface Analysis, 2004, 36, 845-848.	0.8	4
149	Surface defects on collection coins of precious metals. Surface and Interface Analysis, 2004, 36, 921-924.	0.8	7
150	Surface characterization of titanium nitride composite coatings fabricated by reactive plasma spraying. Surface and Interface Analysis, 2004, 36, 1147-1150.	0.8	15
151	Comparison of ZrxTi1â^'xO4 films produced by PLD and MOCVD techniques. Surface and Interface Analysis, 2004, 36, 1151-1154.	0.8	2
152	Deposition and characterization of ZrTiO4 thin films. Surface and Interface Analysis, 2004, 36, 1159-1162.	0.8	17
153	Facile Synthesis and Characterization of Newl <sup>2</sup> -Diketonate Silver Complexes. Single-Crystal Structures of (1,1,1,5,5,5-Hexafluoro-2,4-pentadionato)(2,2â€ <sup>2</sup> -bipyridine)silver(I) and (1,1,1,5,5,5-Hexafluoro-2,4-pentadionato)(N,N,Nâ€ <sup>2</sup> ,Nâ€ <sup>2</sup> -tetramethylethylenediamine)silver(I) and Their Use as MOCVD Precursors for Silver Films. Chemical Vapor Deposition. 2004. 10. 207-213.	1.4	27
154	Characterization of Ga2O3 based MRISiC hydrogen gas sensors. Sensors and Actuators B: Chemical, 2004, 103, 129-135.	4.0	59
155	Determination of vanadium valence in hydrated compounds. Journal of Alloys and Compounds, 2004, 382, 239-243.	2.8	20
156	XPS STUDY OF THIN FILMS OF BINARY METAL OXIDES FOR GAS-SENSING APPLICATIONS. , 2004, , .		0
157	INFLUENCE OF ELECTRODES AGING ON THE RESPONSES OF SNO2 SOL-GEL SENSORS. , 2004, , .		0
158	Sol–gel synthesis and XPS characterization of sodium–vanadium oxide bronze thin films. Journal of Electron Spectroscopy and Related Phenomena, 2003, 131-132, 99-103.	0.8	38
159	Investigation of sol–gel prepared Ga–Zn oxide thin films for oxygen gas sensing. Sensors and Actuators A: Physical, 2003, 108, 263-270.	2.0	34
160	Composition influence on the properties of sputtered Snî—,Wî—,O films. Sensors and Actuators B: Chemical, 2003, 89, 225-231.	4.0	19
161	Investigation of sol–gel prepared CeO2–TiO2 thin films for oxygen gas sensing. Sensors and Actuators B: Chemical, 2003, 95, 145-150.	4.0	90

162 Microstructural Analysis of Ga-Zn Oxide Thin Films for Gas Sensing. , 2003, , .

0

#	Article	IF	CITATIONS
163	Influence of surface properties on the metal oxide sensor response to a steep change in air composition. , 2003, , .		0
164	Microstructure and Magnetotransport Properties of Nanocrystalline Laser Processed Co-Ag Films. Journal of Metastable and Nanocrystalline Materials, 2002, 12, 111-125.	0.1	1
165	Investigation of Pt/Ga 2 O 3 -ZnO/SiC Schottky-diode-based hydrocarbon gas sensors. , 2002, , .		1
166	Thermal treatment stabilization processes in SnO/sub 2/ thin films catalyzed with Au and Pt. IEEE Sensors Journal, 2002, 2, 102-106.	2.4	12
167	Surface study of thin film gas sensors on a Si micro-machined substrate. Applied Surface Science, 2002, 189, 39-52.	3.1	5
168	XPS characterization of biocompatible hydroxyapatite-polymer coatings. Surface and Interface Analysis, 2002, 34, 45-49.	0.8	46
169	Investigation of thin films of mixed oxides for gas-sensing applications. Surface and Interface Analysis, 2002, 34, 672-676.	0.8	37
170	Study of Zr1?xSnxTiO4 thin films prepared by a polymeric precursor route. Surface and Interface Analysis, 2002, 34, 690-693.	0.8	10
171	SENSITIVITY AND SELECTIVITY ENHANCEMENT IN WO3 AND CR2-xTIxO3 THIN FILMS DEPOSITED BY PULSED LASER ABLATION. , 2002, , .		1
172	INFLUENCE OF TECHNOLOGY ON THE TRANSIENT RESPONSE IN METAL OXIDE THIN FILM GAS SENSORS. , 2002, , .		0
173	XPS study of vanadium–yttrium hydrates. Journal of Electron Spectroscopy and Related Phenomena, 2001, 120, 131-135.	0.8	36
174	Properties of CuxS thin film based structures: influence on the sensitivity to ammonia at room temperatures. Thin Solid Films, 2001, 391, 275-281.	0.8	104
175	XPS characterisation of iron-modified vanadyl phosphate catalysts. Applied Catalysis A: General, 2001, 218, 129-137.	2.2	22
176	Hydroxy- and fluorapatite films on Ti alloy substrates: Sol-gel preparation and characterization. Journal of Materials Science, 2001, 36, 3253-3260.	1.7	58
177	Influence of Si, Ni and Co additions on gold alloy for investment cast process. Journal of Alloys and Compounds, 2001, 325, 252-258.	2.8	4
178	Surface studies of in vitro biocompatibility of titanium oxide coatings. Applied Surface Science, 2001, 172, 167-177.	3.1	74
179	The room temperature ammonia sensor based on improved CuxS-micro-porous-Si structure. Sensors and Actuators B: Chemical, 2001, 78, 208-215.	4.0	24
180	Verification of Layered Structures in SnO2/Metal-based Gas Sensors by X-ray Microanalysis: Comparison with X-ray Photoelectron Spectroscopy. Microscopy and Microanalysis, 2001, 7, 518-525.	0.2	0

#	Article	IF	CITATIONS
181	ROOM-TEMPERATURE AMMONIA SENSOR BASED ON <font>Cu</font> <sub><font>x</font><font>S</font> FILM. , 2000, , .</sub>		0
182	XPS and electrochemical characterization of tarnish films on dental alloys. Surface and Interface Analysis, 2000, 30, 50-55.	0.8	6
183	Characterization of thin-film devices for gas sensing. Surface and Interface Analysis, 2000, 30, 502-506.	0.8	24
184	Surface characterization of biocompatible hydroxyapatite coatings. Surface and Interface Analysis, 2000, 29, 773-781.	0.8	49
185	Great reduction of particulates in pulsed laser deposition of Ag–Co films by using a shaded off-axis geometry. Applied Surface Science, 2000, 156, 143-148.	3.1	27
186	Surface chemical composition of MV10Mo2O31·nH2O (M=Na2, K2, Ca, Sr, Cu) xerogels. Journal of Electron Spectroscopy and Related Phenomena, 2000, 107, 253-259.	0.8	7
187	Sol-gel derived hydroxyapatite coatings on titanium substrate. Journal of Materials Science, 2000, 35, 2791-2797.	1.7	127
188	Surface characterization of biocompatible hydroxyapatite coatingsâ€. , 2000, 29, 773.		1
189	TiPc2/Pt ULTRA-THIN FILM SANDWICH STRUCTURE FOR LOW TEMPERATURE GAS SENSOR. , 2000, , .		0
190	Thickness effect of constituent layers on gas sensitivity in SnO2/[metal]/metal multi-layers. Sensors and Actuators B: Chemical, 1999, 58, 478-485.	4.0	7
191	WC–Co cutting tool surface modifications induced by pulsed laser treatment. Applied Surface Science, 1999, 138-139, 376-382.	3.1	35
192	XPS study of ceramic three-way catalysts. Applied Surface Science, 1999, 144-145, 390-394.	3.1	15
193	XPS study of apatite-based coatings prepared by sol–gel technique. Applied Surface Science, 1999, 151, 1-5.	3.1	147
194	Surface Microstructure and Magnetic Properties of Laser-Processed Granular Co-Ag Films. Materials Research Society Symposia Proceedings, 1999, 562, 75.	0.1	1
195	Influence of Cu overlayer on the properties of SnO2-based gas sensors. Thin Solid Films, 1998, 315, 310-315.	0.8	17
196	Stability and oxidation of the sandwich type gas sensors based on thin metal films. Sensors and Actuators B: Chemical, 1998, 48, 376-382.	4.0	7
197	Surface analysis of biocompatible coatings on titanium. Journal of Electron Spectroscopy and Related Phenomena, 1998, 95, 61-69.	0.8	92
198	Peculiarities of surface doping with Cu in SnO2 thin film gas sensors. Sensors and Actuators B: Chemical, 1997, 43, 140-146.	4.0	43

#	Article	IF	CITATIONS
199	Gas induced resistance response in ultra-thin metal films covered with non-conductive layers. Sensors and Actuators B: Chemical, 1997, 43, 186-192.	4.0	3
200	Interaction of mercury vapour with thin films of gold. Applied Surface Science, 1996, 103, 107-111.	3.1	49
201	Interface abruptness in strained III–V heterostructures. Applied Surface Science, 1996, 104-105, 652-655.	3.1	0
202	Investigation of Interface Abruptness in Strained InAs/In <sub>0.53</sub> Ga <sub>0.47</sub> As Quantum Wells. Materials Science Forum, 1996, 203, 231-236.	0.3	0
203	Noise removal from Auger images by using adaptive binomial filter. Journal of Electron Spectroscopy and Related Phenomena, 1995, 76, 399-404.	0.8	8
204	Temperature dependencies of sensitivity and surface chemical composition of SnOx gas sensors. Sensors and Actuators B: Chemical, 1995, 25, 516-519.	4.0	32
205	Influence of chemical composition on sensitivity and signal reproducibility of CdS sensors of oxygen. Sensors and Actuators B: Chemical, 1995, 25, 628-630.	4.0	19
206	Role of the substrate deoxidation process in the growth of strained InAs/InP heterostructures. Journal of Crystal Growth, 1995, 150, 123-127.	0.7	6
207	Surface chemistry of tin oxide based gas sensors. Journal of Applied Physics, 1994, 76, 4467-4471.	1.1	137
208	Characterization study of strained InxGa1â^'xAs/GaAs superlattices. Journal of Applied Physics, 1994, 76, 5738-5743.	1.1	2
209	Surface spectroscopy study of CdSe and CdS thin-film oxygen sensors. Sensors and Actuators B: Chemical, 1994, 22, 189-194.	4.0	10
210	Investigation of CdS passivation layers on Hg1â^'xCdxTe. Surface and Interface Analysis, 1994, 22, 197-201.	0.8	3
211	Characterization study of CdS passivation layers on. Materials Science and Engineering B: Solid-State Materials for Advanced Technology, 1994, 28, 43-46.	1.7	2
212	Depth profiling of InAs/InP and heterostructures grown by molecular beam epitaxy. Materials Science and Engineering B: Solid-State Materials for Advanced Technology, 1994, 28, 228-231.	1.7	2
213	Photoelectron spectroscopy of the poly-vanadium transition metal acids. Applied Surface Science, 1994, 78, 107-112.	3.1	11
214	XPS study of the InxGa1â^'xAsGaAs superlattice. Journal of Electron Spectroscopy and Related Phenomena, 1994, 70, 145-149.	0.8	7
215	Valence band states of H:GaAs(110). Surface Science, 1994, 307-309, 890-895.	0.8	13
216	Depth profiling of InxGa1-xAs/GaAs superlattice. Applied Surface Science, 1993, 72, 89-93.	3.1	8

#	Article	IF	CITATIONS
217	Investigation of Yî—,Tbî—,Baî—,Cuî—,O compounds by XPS. Surface Science, 1992, 269-270, 1077-1081.	0.8	2
218	Rare-earth sesquisulphides investigation by ELS and XPS. Surface Science, 1991, 251-252, 330-335.	0.8	35
219	AES depth profile study of a GaAs/AlAs superlattice. Surface and Interface Analysis, 1991, 17, 816-818.	0.8	5
220	Dependence of I-U Characteristics of GaAs n+-n-n+ Diodes on the Active Region Length. Physica Status Solidi A, 1984, 85, K179-K182.	1.7	4
221	Thin films of Zr/sub 1-x/Sn/sub x/TiO/sub 4/ for application in microelectronics. , 0, , .		Ο
222	Mixed Oxide Pt/(Ti-W-O)/SiC Based MROSiC Device for Hydrocarbon Gas Sensing. , 0, , .		0
223	Long-Term Heat Treatments on Ti6Al4V-SiC <sub>f</sub> Composite. Part I - Microstructural Characterization. Materials Science Forum, 0, 604-605, 331-340.	0.3	5
224	Microstructural Characterization of Ti6Al4V-SiC <sub>f</sub> Composite Produced by New Roll-Bonding Process. Advanced Materials Research, 0, 89-91, 715-720.	0.3	2
225	Micro-Chemistry and Mechanical Behaviour of Ti6Al4V-SiC <sub>f</sub> Composite Produced by HIP for Aeronautical Applications. Materials Science Forum, 0, 678, 23-47.	0.3	3
226	Young's Modulus Profile in Kolsterized AISI 316L Steel. Materials Science Forum, 0, 762, 183-188.	0.3	20
227	Elemental Clustering and Structure of Liquid LBE. Advanced Materials Research, 0, 922, 785-790.	0.3	0
228	Temperature Dependent Phenomena in Liquid LBE Alloy. Materials Science Forum, 0, 884, 41-52.	0.3	3